


Article

Research on Combustion Characteristics of Air–Light Hydrocarbon Mixing Gas

Zhiqun Meng , Jinggang Wang *, Chuchao Xiong, Jiawen Qi and Liquan Hou

School of Energy and Environmental Engineering, Hebei University of Engineering, Handan 056038, China; fanzqmeng@163.com (Z.M.); xiongchuchao@126.com (C.X.); jiawenqi1001@163.com (J.Q.); houliquan@sina.com (L.H.)

* Correspondence: jinggangwang@hebeu.edu.cn

Received: 26 May 2020; Accepted: 19 June 2020; Published: 24 June 2020



Abstract: Air–light hydrocarbon mixing gas is a new type of city gas which is composed of light hydrocarbon with the main component of *n*-pentane and air mixed in a certain proportion. To explore the dominant reactions for CO production of air–light hydrocarbon mixing gas with different mixing degrees at the critical equivalence ratios, a computational study was conducted on the combustion characteristics, including the ignition delay time, laminar flame speed, extinction residence time, and emission of air–light hydrocarbon mixing gas at atmospheric pressure and room temperature in the present study. The calculated results indicate that the ignition delay time of air–light hydrocarbon mixing gas at temperatures of 1000–1118 K is greater than that of *n*-pentane, while the opposite at temperatures of 1118–1600 K. From the study of the laminar flame speed and ignition delay time, it was found that the essence of air–light hydrocarbon mixing gas is that its attribute parameter is determined by the ratio of *n*-pentane to the total amount of air at the moment of combustion. The changes in the extinction residence time and the CO emission index of air–light hydrocarbon mixing gas are not synchronized, that is the CO emission index is not necessarily small for air–light hydrocarbon mixing gas with excellent extinction residence time. CO sensitivity analysis and CO rate of production identified key species and reactions that are primarily responsible for CO formation and annihilation. The mixing degree plays a key role in the CO emission index of air–light hydrocarbon mixing gas, which has a constructive opinion on the future experiment and application of air–light hydrocarbon mixing gas.

Keywords: air–light hydrocarbon mixing gas; *n*-pentane; ignition delay time; laminar flame speed; extinction residence time; emission

1. Introduction

Energy is the key to global prosperity, well-being, and the foundation of human life and industrial activities. With the rapid growth of the global economy and the increasing demand for heating and cooling in certain parts of the world, according to statistics from the International Energy Agency (IEA), global energy consumption increased by 2.3% year-on-year in 2018, almost twice the average growth rate since 2010 [1]. In recent years, global energy supply and demand and governance methods have undergone profound changes, and major countries and regions in the world have also adjusted their mid- and long-term energy development strategies in a timely manner [2–4]. China, on the one hand, is actively constructing new energy structures, such as the development of wind energy, water energy, nuclear energy, and geothermal energy; on the other hand, it is seeking the comprehensive utilization of traditional energy, that is the mode of energy utilization is changing from extensive to intensive, such as recycling by-products generated during oilfield mining. Part of these recovered by-products can be separated to extract a light hydrocarbon with the main component of *n*-pentane,

abbreviated as light hydrocarbon. The researchers found that the light hydrocarbon that appears in liquid form at atmospheric pressure can burn as a fuel after being gasified and mixed with air at an appropriate ratio. It has high calorific value, high utilization rate, and can be used as an independent gas source, which is very suitable as urban gas [5]. This mixed gas is called as air–light hydrocarbon mixing gas. In 2010, China issued the “air–light hydrocarbon mixing gas” standard, which identified the air–light hydrocarbon mixing gas as the “Fourth Urban Gas” after artificial gas, natural gas, and liquefied petroleum gas. This means that air–light hydrocarbon mixing gas will play an important role in China’s future energy structure.

Since air–light hydrocarbon mixing gas has been approved, the related theoretical research has been further deepened. Fan et al. explored mixed parameters, explosion limits and safety issues. However, this level of research is far from enough for a new type of urban gas [6–8]. For the exploration, experiment, simulation, and engineering practice of a kind of fuel, the relevant researches of natural gas have great reference value. Xie et al. [9] conducted experiments and numerical studies on the laminar flame characteristics of a highly diluted $\text{CH}_4/\text{CO}_2/\text{O}_2$ mixtures using a constant volume chamber and CHEMKIN. The results showed that carbon dioxide suppresses the instability of the methane flame. Hu et al. [10] conducted experiments and numerical studies on the laminar combustion characteristics of a methane–hydrogen–air premixed flame at room temperature and atmospheric pressure. The results indicated that, as the hydrogen content increases, the unstretched laminar burning velocity increases, and the peak of the unstretched laminar burning velocity moves toward the mixture enrichment side. Brower et al. [11] calculated the ignition delay time and laminar flame speed of fuels from pure methane to pure hydrogen and natural gas–hydrogen mixtures using highly optimized chemical kinetic mechanisms. The results showed that, by increasing the laminar flame speed and reducing the ignition delay time, the reactivity of the hydrocarbon fuel under all conditions can be improved. Wang et al. [12] used the PREMIX code of the CHEMKIN II program with the GRI-Mech 3.0 mechanism to calculate the laminar premixed flame of methane–hydrogen–air stoichiometric methane free diffusion at room temperature and pressure. The results indicated that, with hydrogen addition, the production rate of the main reactions contributing to CH_4 , CO and CO_2 shows a significant increase. Hu et al. [13] optimized the global reaction mechanism of methane under MILD conditions. Comparing the optimized and other global mechanisms through the methods of computational fluid dynamics and a plug flow reactor, they found that the optimized global mechanism greatly improves the temperature, the equilibrium concentration of the main substances, and the prediction of the peak CO concentration. Liu et al. [14] used the CHEMKIN 2.0 code with an improved GRI-Mech 3.0 mechanism to numerically study the chemical, thermal, and diffusion effects of hydrogenation and carbon monoxide on the methane laminar flame characteristics. The results showed that the effect of hydrogen addition on the laminar flame velocity is mainly under lean and stoichiometric conditions. Karyeyen [15] studied the combustion characteristics of the non-premixed methane flame of the new burner under conventional and distributed combustion conditions. The results indicated that distributed combustion can achieve a more uniform thermal field, and the pollutant emissions from distributed combustion have been reduced to near zero emissions. Yan et al. [16] proposed a new opposed counter-flow micro-combustor with a special multi-stage separation baffle and compared it with two other conventional micro-combustors. Through the numerical simulation study of methane in three types of combustors, they found that the new type of combustor is better than ordinary combustors in terms of combustion efficiency, extended intake speed limit and thermal cycle. Chen et al. [17] used a two-dimensional chemical fluid dynamics model to study the combustion characteristics and stability of methane–air mixtures on platinum in catalytic micro-combustors. The results showed that the size of the combustion chamber is critical to determine the combustion stability of the system. Xiao et al. [18] developed a detailed chemical kinetic mechanism model of the ammonia–methane mixed fuel to simulate its combustion characteristics. By analyzing the ignition delay time and laminar flame structure, they found that harmful emissions can be significantly reduced. Ku et al. [19] conducted

experimental and computational studies on the basic combustion characteristics of methane–ammonia mixtures, developed a new reaction mechanism, and optimized it.

In summary, methane research is very extensive and in-depth, including the improvement and optimization of kinetic mechanisms, experiments and simulations of premixed combustion characteristics, and the exploration and innovation of combustion methods and combustors. These series of studies are of great significance to the promotion and application of natural gas. For, the research on *n*-pentane is analyzed. Pilcher and Chadwick [20] measured the heat of gaseous combustion of pentane isomers at a temperature of 298 K and a pressure of 1 atm. Knox and Kinnear [21] studied the initial stage of the slow reaction of gaseous *n*-pentane with oxygen under static conditions of 523–673 K. Hughes et al. [22] studied the reaction of *n*-pentane with oxygen in the temperature range of 530–553 K, including the slow oxidation zone and the cold flame zone. Westbrook et al. [23] used a numerical model and a detailed chemical kinetic reaction mechanism to study the oxidation reaction of *n*-pentane in a stirred reactor, including 53 chemical species and 326 basic reactions. Chakir et al. [24] studied the oxidation reaction of *n*-pentane in a jet-stirred reactor in the temperature range of 950–1050 K, which is suitable for a wide range of fuel–oxygen equivalent ratios (0.2–2.0). Zhukov et al. [25] determined the ignition delay time of *n*-pentane when the equivalence ratio was 0.5, the temperature was 867–1534 K, and the pressure was 11–530 atm. Bugler et al. [26,27] studied the ignition delay time of *n*-pentane in two shock tubes and the chemical products of the oxidation process of *n*-pentane in two jet-stirred reactors under a wide range of temperatures and pressures. Kelley et al. [28] innovatively designed the high temperature, high pressure, and constant pressure combustion chamber environment to determine the experimental data of the laminar flame speed of C₅ to C₈ *n*-alkanes. It can be seen that the practical application research of *n*-pentane is lacking, and the study of air–light hydrocarbon mixing gas can fill this gap.

The research history of methane indicates that using the detailed mechanism of a fuel to study its characteristic parameters is indispensable. Therefore, the purpose of this study was to investigate the combustion reaction characteristics, including the ignition delay time, laminar flame speed, extinction residence time, and emission of air–light hydrocarbon mixing gas with different mixing degrees at the critical equivalence ratios. The present study provides effective reference suggestions for the next experiments of air–light hydrocarbon mixing gas and has practical significance for the rich study of the air–fuel mixed combustion characteristics of hydrocarbon fuels.

According to the extensive research on *n*-pentane by Jiang et al. [29], the pentane isomer model of National University of Ireland, Galway has a better agreement with the experimental results. Thus, the NUI Galway pentane isomer model, including 697 species and 3214 reactions, was selected as the detailed chemical mechanism for *n*-pentane, which was the base fuel in this study.

2. Numerical Models and Computational Cases

2.1. Numerical Models

The ignition delay time is determined by the closed homogeneous batch reactor model in ANSYS CHEMKIN 17.0 [30] at temperatures of 1000–1600 K and a pressure of 1 atm. According to the experiment of Bugler et al., the ignition delay time is defined as auto-ignition.

The laminar flame speed is calculated at a pressure of 1 atm by using the premixed laminar flame-speed calculation model in ANSYS CHEMKIN 17.0 [30]. The unburned gas temperature is mentioned in the specific simulation calculation below.

The calculation of extinction residence time and emission at a pressure of 1 atm and an inlet temperature of 298 K is performed using the perfectly stirred reactor (PSR) provided by ANSYS CHEMKIN 17.0 [30]. It is assumed that the mixing is infinitely fast and the extinction is achieved by reducing the residence time until there is not enough time to react in a PSR [31,32]. As a civilian fuel, the CO produced by air–light hydrocarbon mixing gas poses a threat to human safety, and the generation of more CO also indicates low combustion efficiency. Thus, to determine the main reaction

for CO production, the sensitivity analysis of CO production and the CO rate of production (ROP) are studied in PSR [33].

2.2. Computational Cases

First, understand the laminar flame speed of *n*-pentane–air at different equivalence ratios, which involves the combustion limit of lean and rich fuel. Figure 1 shows the laminar flame speeds of *n*-pentane–air at equivalent ratios of 0.4–2.5 and unburned gas temperatures of 298, 353, and 400 K, respectively. The experimental data were measured by Kelley et al. [28] at an unburned gas temperature of 353 K. As can be seen, no matter what kind of unburned gas temperature, the laminar flame speed is close to 0 cm/s when the equivalent ratio is 0.4 or 2.5. In particular, the unburned gas temperature in this study is 298 K, and the investigated range of equivalent ratio is 0.4–2.5.

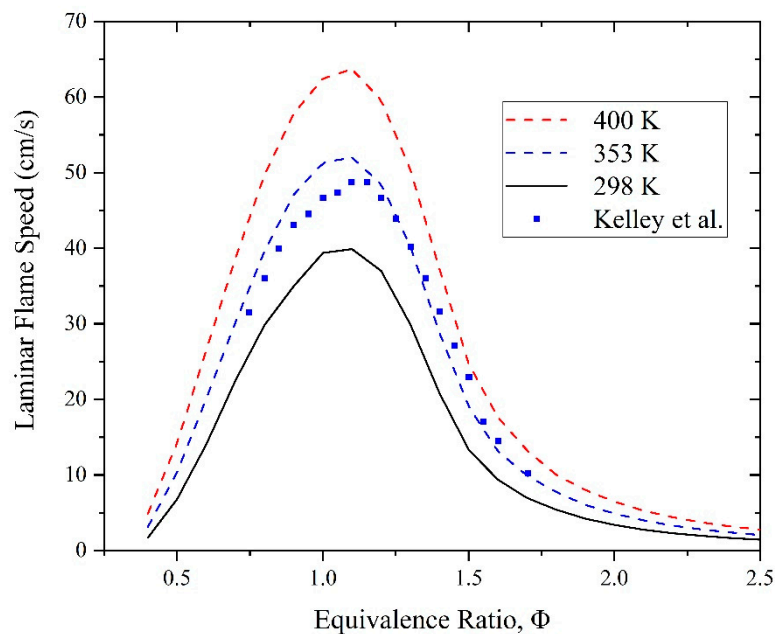


Figure 1. The laminar flame speed of *n*-pentane–air at equivalent ratios of 0.4–2.5 and unburned gas temperatures of 298, 353, and 400 K, respectively.

Next, the essence of air–light hydrocarbon mixing gas is *n*-pentane mixed with air in a certain ratio, and then it is regarded as a whole fuel. According to the research of Fan et al. on air–light hydrocarbon mixing gas, the mixing degree of *n*-pentane and air is defined as:

$$Z = 1: n, n = 1, 2, 3, 4 \quad (1)$$

that is, 1 mol of *n*-pentane mixed with *n* mol of air is the air–light hydrocarbon mixing gas with a mixing degree of *Z*. This indicates that air–light hydrocarbon mixing gas is a dilution of *n*-pentane. Therefore, when air–light hydrocarbon mixing gas reacts with air, the above-mentioned laminar flame speed problem of lean and rich fuel must be considered. Table 1 summarizes the computational cases of air–light hydrocarbon mixing gas and air combustion. All data of computational cases were obtained based on the above situation combined with the actual project. Although there may be slight deviations in the calculation results, the retention of 6 or 7 decimal places is considered according to specific cases, so that the accuracy can be improved as much as possible. The equivalent ratio refers to the equivalent ratio of *n*-pentane to air. $1/Z_{\Phi}$ refers to the reciprocal of *Z* at Φ . For example, the equivalent ratio of *n*-pentane to air is 1.2, thus the maximum mixing degree of *n*-pentane and air can only reach $Z_{1.2} = 1:2 = 1/2$, i.e., $1/Z_{1.2} = 2$. In this way, the specific mole fractions of *n*-pentane, nitrogen, and oxygen when air–light hydrocarbon mixing gas and air are combusted at this mixing degree can

be obtained. $1/Z_{\Phi} = 0$ means pure *n*-pentane without mixed air, in order to provide reference data. After many simulation tests of the laminar flame speed, the equivalent ratios of 0.8, 1.2, 1.7, and 2.1 correspond to the maximum mixing degree of *n*-pentane and air of 1, 1/2, 1/3, and 1/4, respectively. It can also be understood that, when the equivalence ratio is less than 0.8, *n*-pentane cannot mix air, and, when the equivalence ratio is greater than 2.1, *n*-pentane can mix air at any mixing degree. However, it should be noted that the final mole fraction of *n*-pentane cannot be higher than the mole fraction of *n*-pentane when the equivalent ratio is 2.5.

Table 1. The computational cases of air–light hydrocarbon mixing gas and air combustion.

Equivalence Ratio, Φ	$1/Z_{\Phi}$	Mole Fraction		
		<i>n</i> -C ₅ H ₁₂	N ₂	O ₂
0.8	0	0.020568	0.773750	0.205682
	1	0.010284	0.781874	0.207842
1.2	0	0.030538	0.765874	0.203588
	1	0.015269	0.777937	0.206794
	2	0.010180	0.781957	0.207863
1.7	0	0.042720	0.7562500	0.2010300
	1	0.021360	0.7731244	0.2055156
	2	0.014240	0.7787492	0.2070108
	3	0.010680	0.7815616	0.2077584
2.1	0	0.0522450	0.7487250	0.1990300
	1	0.0261225	0.7693618	0.2045157
	2	0.0174150	0.7762410	0.2063440
	3	0.0130610	0.7796800	0.2072590
	4	0.0104490	0.7817440	0.2078070

3. Results and Discussions

3.1. Ignition Delay Time

Figures 2–5 show ignition delay times of air–light hydrocarbon mixing gas at different mixing degrees and *n*-pentane at equivalent ratios of 0.5, 1.2, 1.7, and 2.1, respectively. As shown in Figure 2, there is a temperature node. When the temperature is lower than this node, the ignition delay time of air–light hydrocarbon mixing gas is longer than that of *n*-pentane. When the temperature is higher than this node, the ignition delay time of air–light hydrocarbon mixing gas is shorter than that of *n*-pentane. There is also a temperature node in Figure 3; the above rule still exists, but it is also found that the smaller is the mixing degree of air–light hydrocarbon mixing gas, the smaller is the ignition delay time. Figures 4 and 5 also obey the above two rules. Next, Figures 2–5 are summarized in a graph to verify whether the temperature nodes that appear in the ignition delay time study of air–mixed light hydrocarbon gas with different mixing degrees are the same.

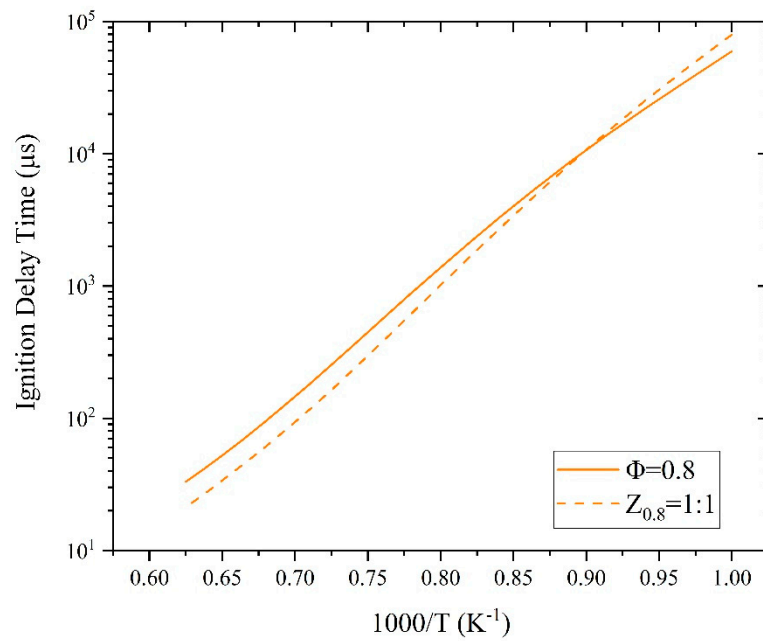


Figure 2. Comparison of the ignition delay times of *n*-pentane at an equivalence ratio of 0.8 and air–light hydrocarbon mixing gas at a mixing degree of 1.

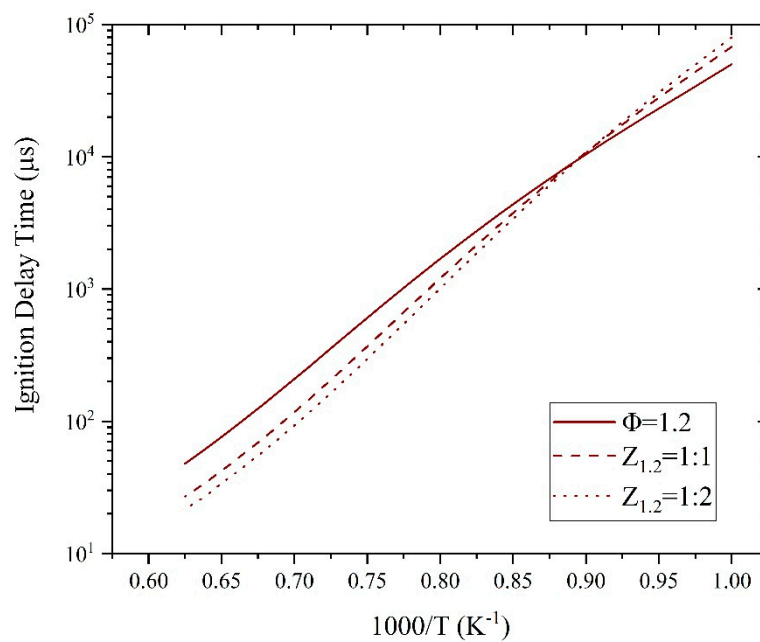


Figure 3. Comparison of the ignition delay times of *n*-pentane at an equivalence ratio of 1.2 and air–light hydrocarbon mixing gas at mixing degree of 1 and 1/2, respectively.

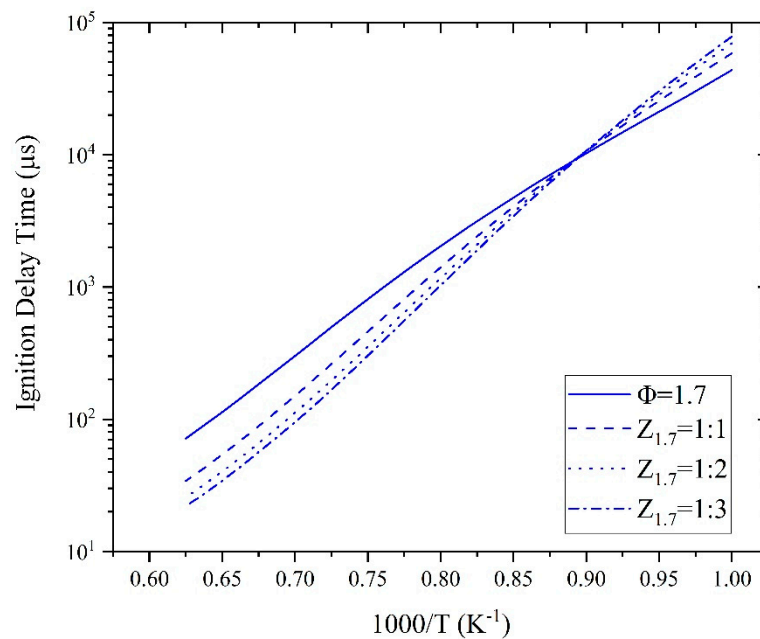


Figure 4. Comparison of the ignition delay times of *n*-pentane at an equivalence ratio of 1.7 and air–light hydrocarbon mixing gas at mixing degree of 1, 1/2, and 1/3, respectively.

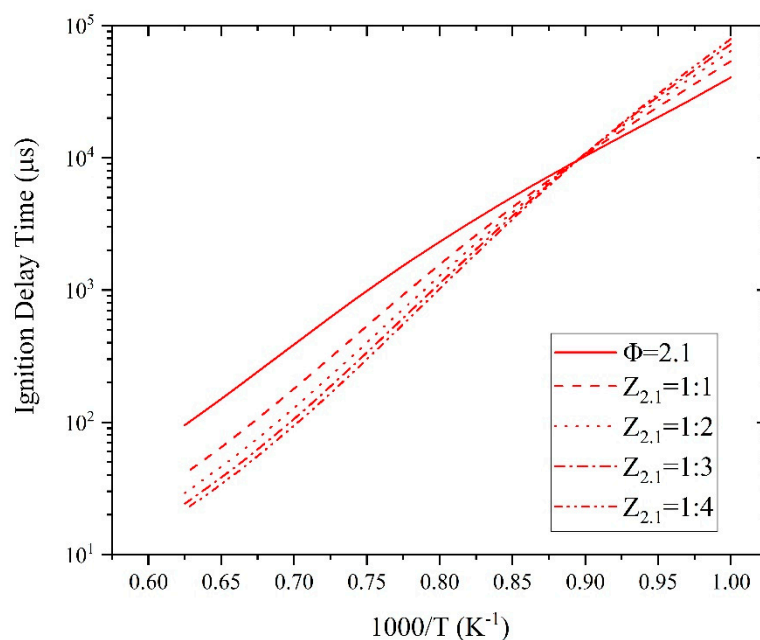


Figure 5. Comparison of the ignition delay times of *n*-pentane at an equivalence ratio of 2.1 and air–light hydrocarbon mixing gas at mixing degree of 1, 1/2, 1/3, and 1/4, respectively.

Figure 6 shows ignition delay times of air–light hydrocarbon mixing gas at different mixing degrees and *n*-pentane at equivalence ratios of 0.8, 1.2, 1.7, and 2.1, respectively. Obviously, the temperature nodes are the same. This temperature node can be calculated to be approximately 1118 K. Then, the above rules are summarized as: in the temperature range of 1000–1118 K, compared with the ignition delay time of *n*-pentane, the smaller is the mixing degree, the longer is the ignition delay time of air–light hydrocarbon mixing gas. In the temperature range of 1118–1600 K, compared with the ignition delay time of *n*-pentane, the smaller is the mixing degree, the shorter is the ignition delay time of air–light hydrocarbon mixing gas. Figure 7 plots the ignition delay time as a function of the reciprocal of the mixing degree at temperatures of 1000 and 1600 K, respectively. Since the four equivalence

ratios selected are the critical values of each mixing degree, the ignition delay time of the maximum mixing degree at each equivalence ratio tends to be the same regardless of the entire temperature line or single temperature point. Expanded, this indicates that the problem of the maximum mixing degree of different equivalence ratios is essentially the problem of the minimum mole fraction required for the combustion reaction of *n*-pentane and air.

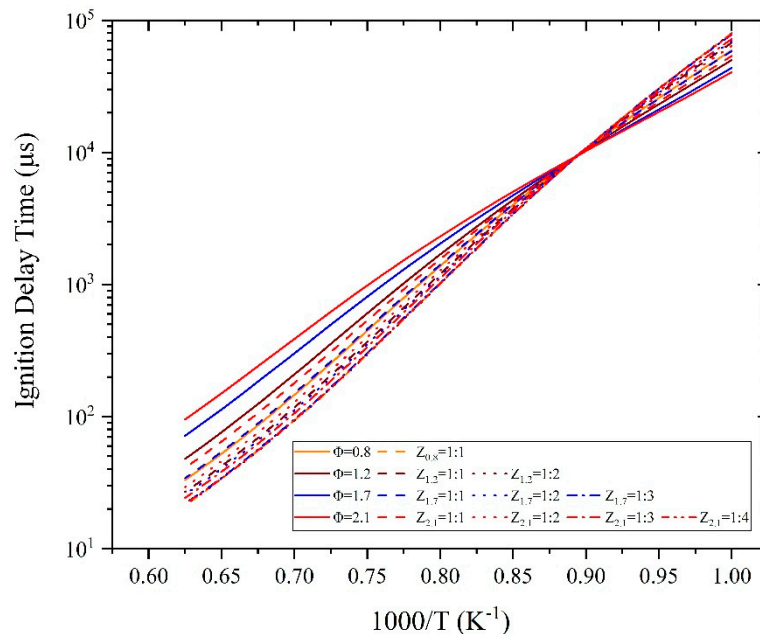


Figure 6. Comprehensive comparison of the ignition delay times of air–light hydrocarbon mixing gas at different mixing degrees and *n*-pentane at equivalence ratios of 0.8, 1.2, 1.7, and 2.1, respectively.

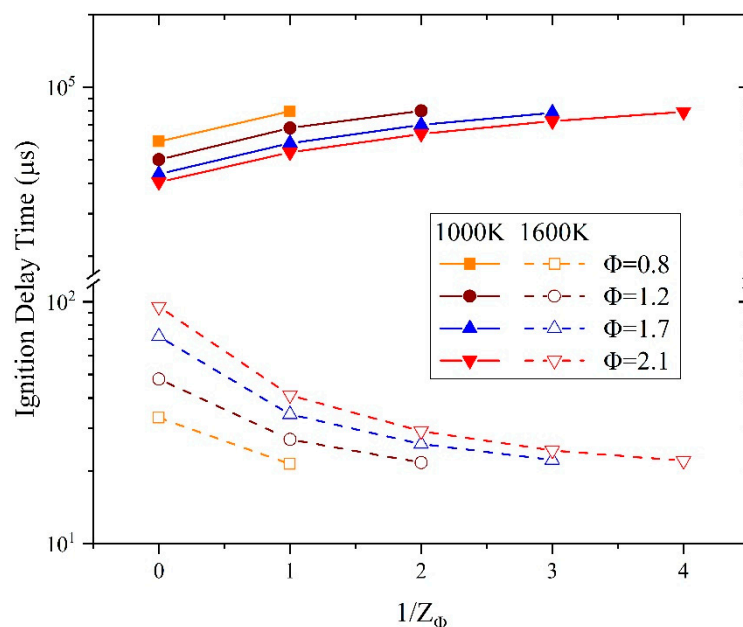


Figure 7. Comparison of the ignition delay times of air–light hydrocarbon mixing gas at the reciprocal of each mixing degree at temperatures of 1000 and 1600 K, respectively.

3.2. Laminar Flame Speed

Figure 8 plots the laminar flame speed as a function of the reciprocal of the mixing degree at an unburned gas temperature of 298 K. Combining with Figure 1, it can be concluded that the laminar

flame speed of air–light hydrocarbon mixing gas changes according to the ratio of the mole fraction of *n*-pentane to the total mole fraction of air. At each equivalence ratio, as shown in Figure 8, the laminar flame speed of the maximum mixing degree tends to be the same. It is further verified that the final conclusion of the ignition delay time study, whether air–light hydrocarbon mixing gas can produce a combustion reaction is fundamentally whether the mole fraction of *n*-pentane in the whole gas at the moment of ignition of air–light hydrocarbon mixing gas is greater than the critical value of the combustion reaction.

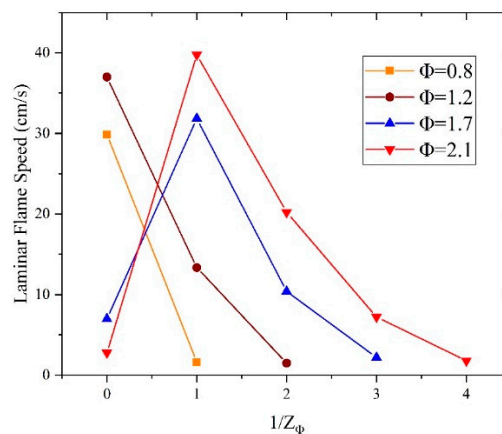


Figure 8. Comparison of the laminar flame speeds of air–light hydrocarbon mixing gas at the reciprocal of each mixing degree at an unburned gas temperature of 298 K.

3.3. Extinction Residence Time and Emission

Figures 9–12 show relationship curves (C-curves) of the residence time and the temperature of air–light hydrocarbon mixing gas at different mixing degrees and *n*-pentane at equivalent ratios of 0.5, 1.2, 1.7, and 2.1, respectively. It can be seen that, in the equivalence ratios where the minimum mixing degree is not less than 1/2, the extinction residence time of air–light hydrocarbon mixing gas is increasing, and, in the equivalence ratios where the minimum mixing degree is not more than 1/3, the extinction residence time of air–light hydrocarbon mixing gas at the minimum mixing degree is decreasing. Figure 13 shows C-curves of air–light hydrocarbon mixing gas at different mixing degrees and *n*-pentane at equivalence ratios of 0.8, 1.2, 1.7, and 2.1, respectively. Within the residence time of 0.1–100 ms, the lower temperature region of C-curves of air–light hydrocarbon mixing gas is approaching a limit. According to the essence of air–light hydrocarbon mixing gas described above, this limit is the limit of the lower temperature region of *n*-pentane lean fuel combustion.

Figure 14 plots the extinction residence time as a function of the reciprocal of the mixing degree and the CO emission indices of the corresponding the reciprocal of the mixing degree at the residence time of 20 ms. The residence time of 20 ms was chosen because it lies between the extinction and equilibrium of all computational cases. The CO emission index refers to the mass ratio of CO generated to fuel reacted in the combustion reaction. Different from the other studied parameter laws, the CO minimum emission index is neither at the minimum mixing degree nor at the maximum mixing degree, but at the position prior to the minimum mixing degree. The most striking contrast is that the reciprocal of the mixing degree is 2, the extinction residence time of B is less than A, but the CO emission index of C is greater than D. In other words, the optimal values of extinction residence time and CO emission index do not overlap. This is one of the key issues to be considered in the research and application of air–light hydrocarbon mixing gas in the future.

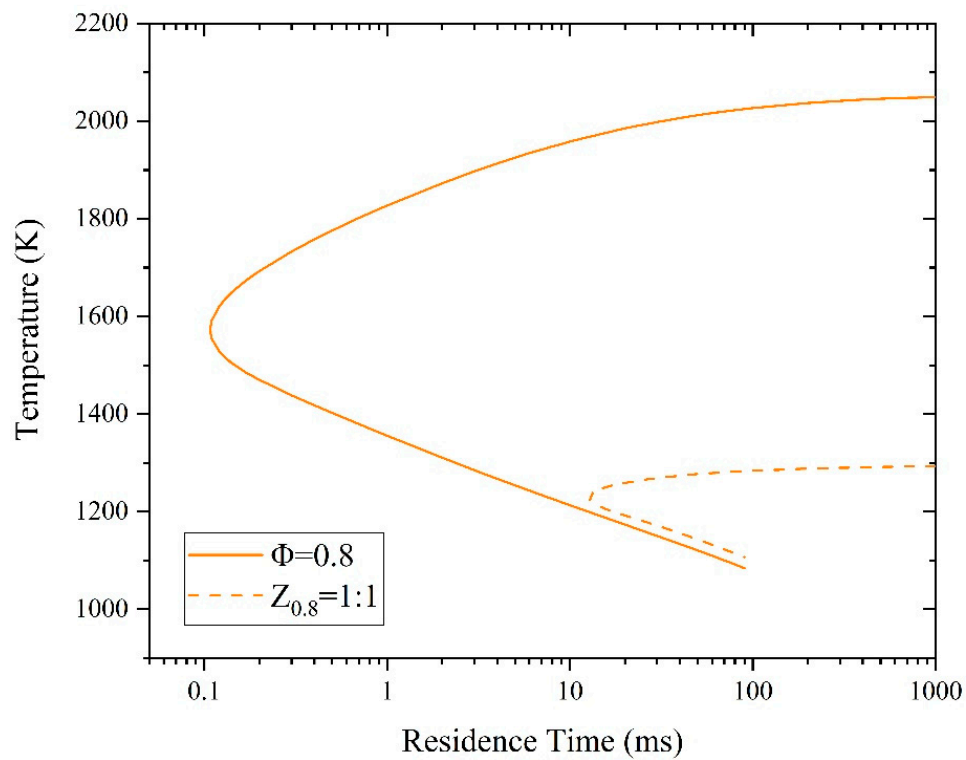


Figure 9. Comparison of C-curves of *n*-pentane at an equivalence ratio of 0.8 and air-light hydrocarbon mixing gas at a mixing degree of 1.

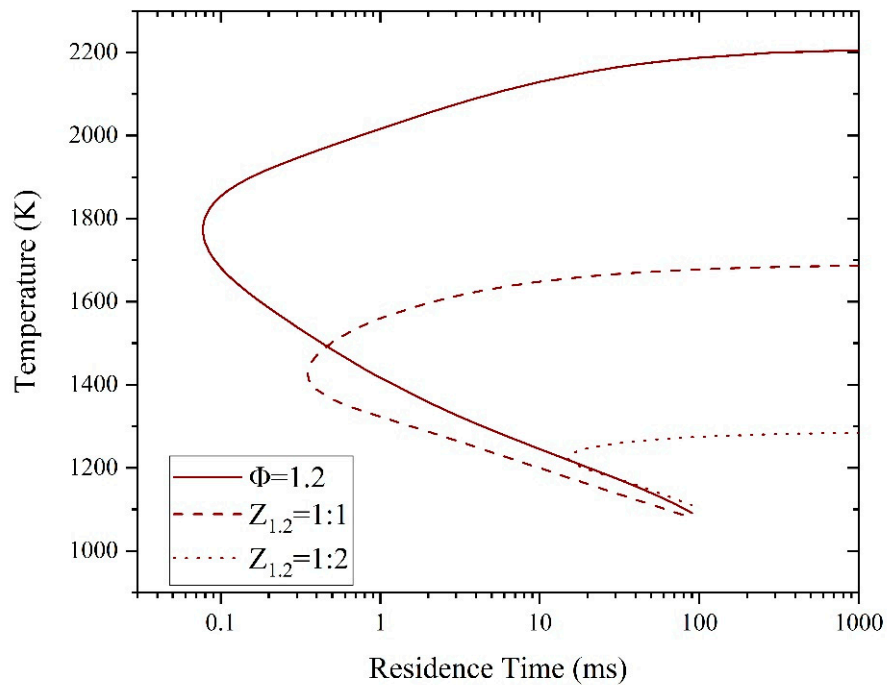


Figure 10. Comparison of C-curves of *n*-pentane at an equivalence ratio of 1.2 and air-light hydrocarbon mixing gas at mixing degree of 1 and 1/2, respectively.

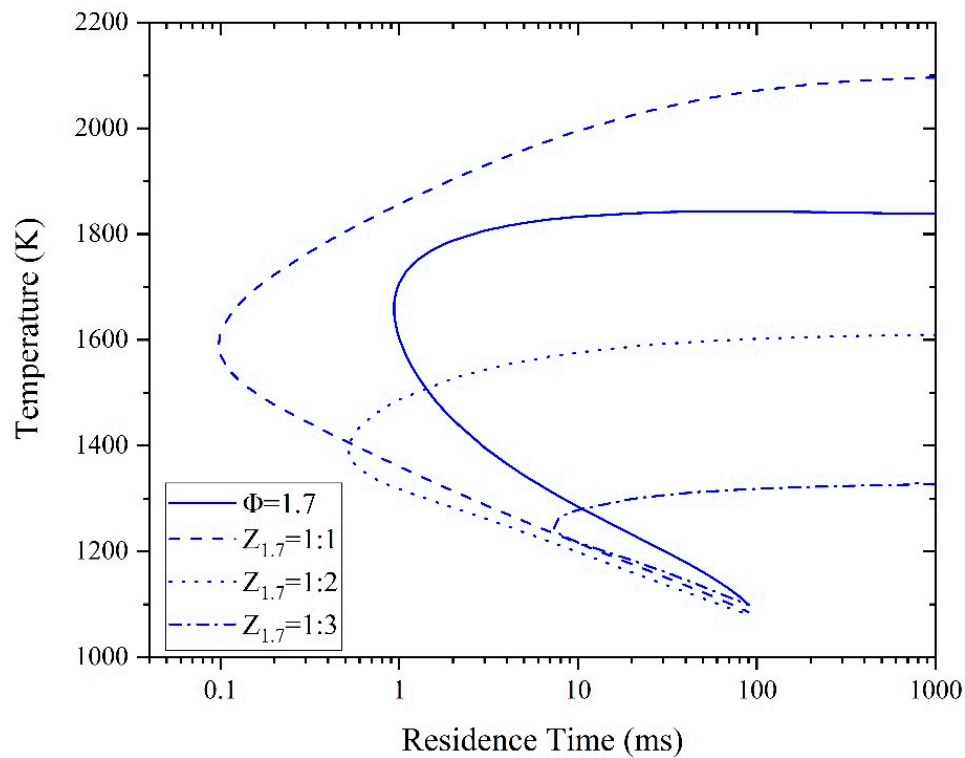


Figure 11. Comparison of C-curves of *n*-pentane at an equivalence ratio of 1.7 and air-light hydrocarbon mixing gas at mixing degree of 1, 1/2, and 1/3, respectively.

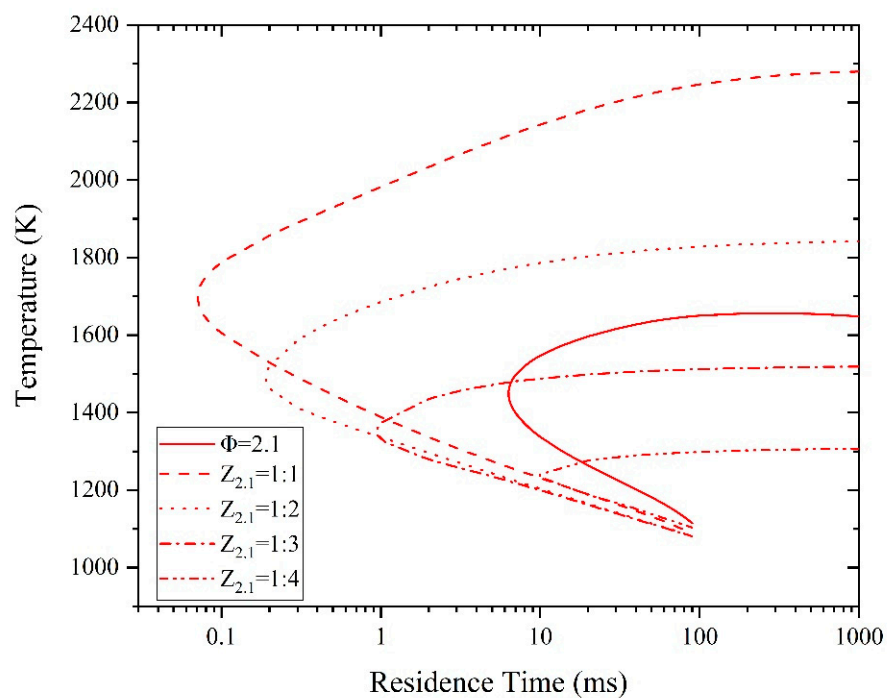


Figure 12. Comparison of C-curves of *n*-pentane at an equivalence ratio of 2.1 and air-light hydrocarbon mixing gas at mixing degree of 1, 1/2, 1/3, and 1/4, respectively.

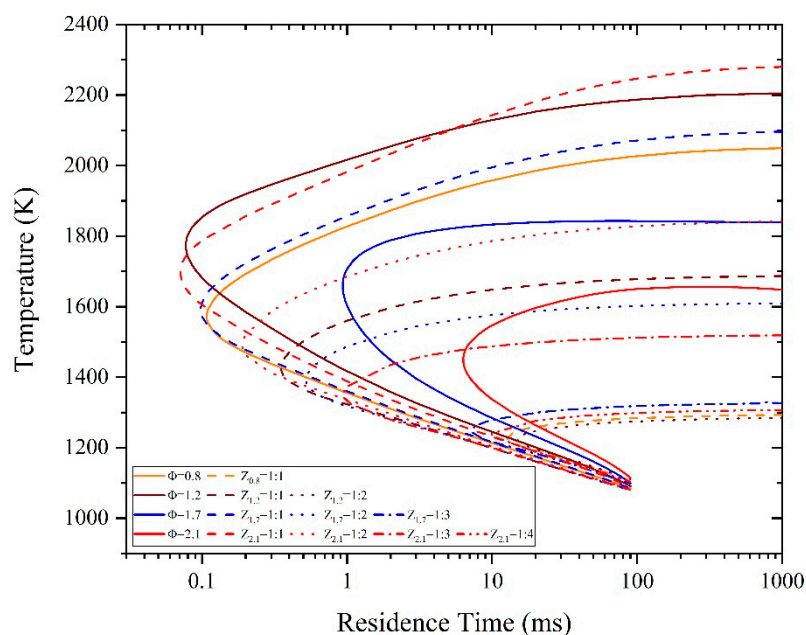


Figure 13. Comprehensive comparison of C-curves of air–light hydrocarbon mixing gas at different mixing degrees and *n*-pentane at equivalence ratios of 0.8, 1.2, 1.7, and 2.1, respectively.

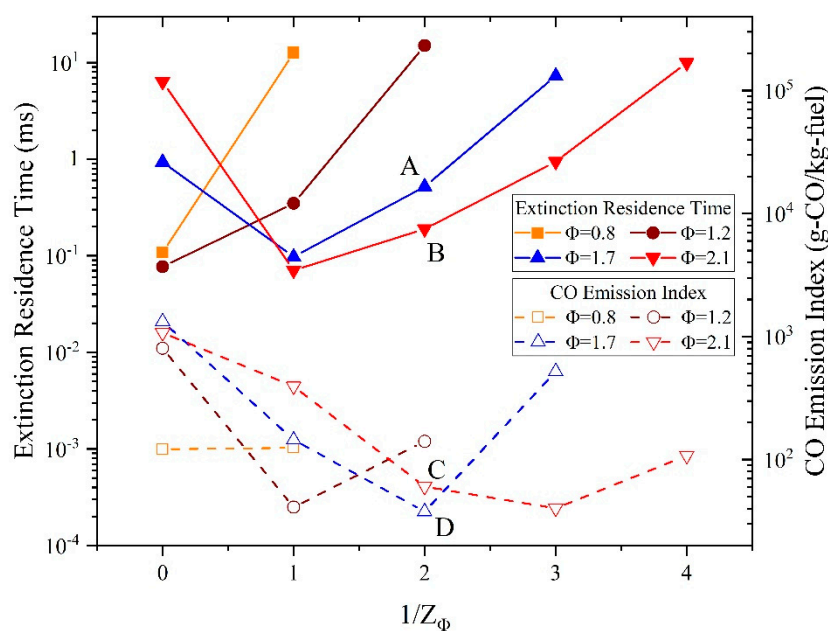


Figure 14. Comparison of the extinction residence times of air–light hydrocarbon mixing gas at the reciprocal of each mixing degree and the CO emission indices corresponding to the residence time of 20 ms.

Figure 15 shows CO sensitivity analysis of air–light hydrocarbon mixing gas at the maximum mixing degree for equivalence ratios of *n*-pentane. Figure 16 shows CO ROP of air–light hydrocarbon mixing gas at the maximum mixing degree for equivalence ratios of *n*-pentane. Table 2 lists the reactions that play important roles in the production and annihilation of CO. Combining the analysis of Figures 15 and 16, the formation of CO in the combustion of air–light hydrocarbon mixing gas is mainly dominated by $\text{HCO} + \text{O}_2 \rightleftharpoons \text{CO} + \text{HO}_2$ (R32). It can also be considered that HCO radicals make the greatest contribution to the formation of CO. The main pathway for the consumption of CO is $\text{CO} +$

OH \rightleftharpoons CO₂ + H (R28), that is CO reacts with OH radicals to finally generate stable CO₂. In particular, when the equivalence ratio is 1.7 and the maximum mixing degree of air–light hydrocarbon mixing gas is 1:3, the most sensitive reaction to CO is H + O₂ \rightleftharpoons O + OH (R1). In connection with the analysis in Figure 14, under this condition, the CO emission index is the highest among air–light hydrocarbon mixing gas, which illustrates that R1 plays a key role in promoting the generation of CO.

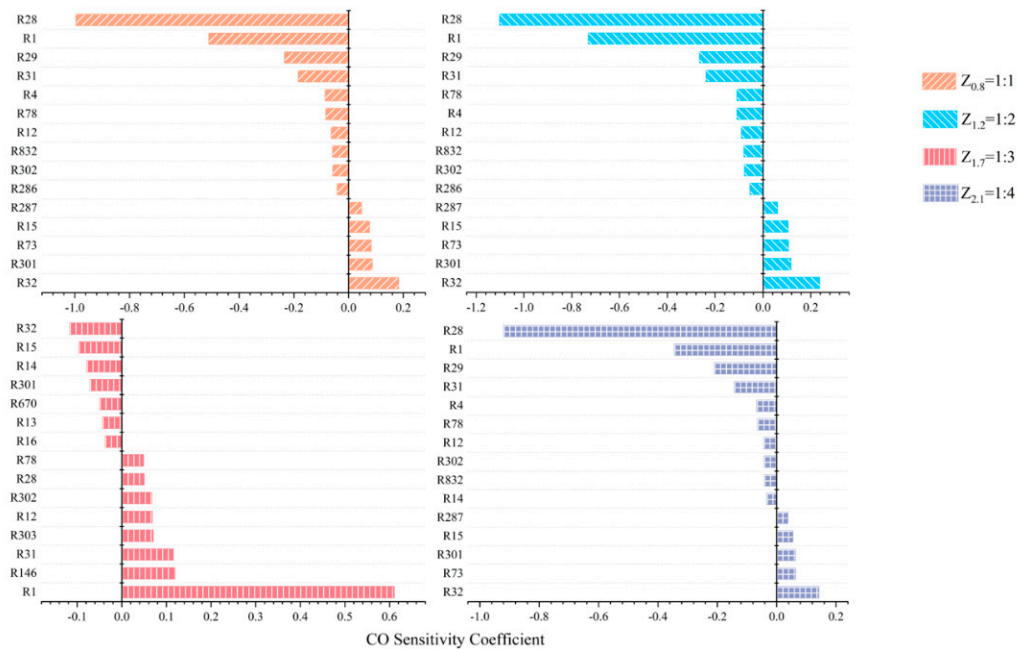


Figure 15. Comprehensive comparison of CO sensitivity analysis of air–light hydrocarbon mixing gas at the maximum mixing degree for equivalence ratios of *n*-pentane.

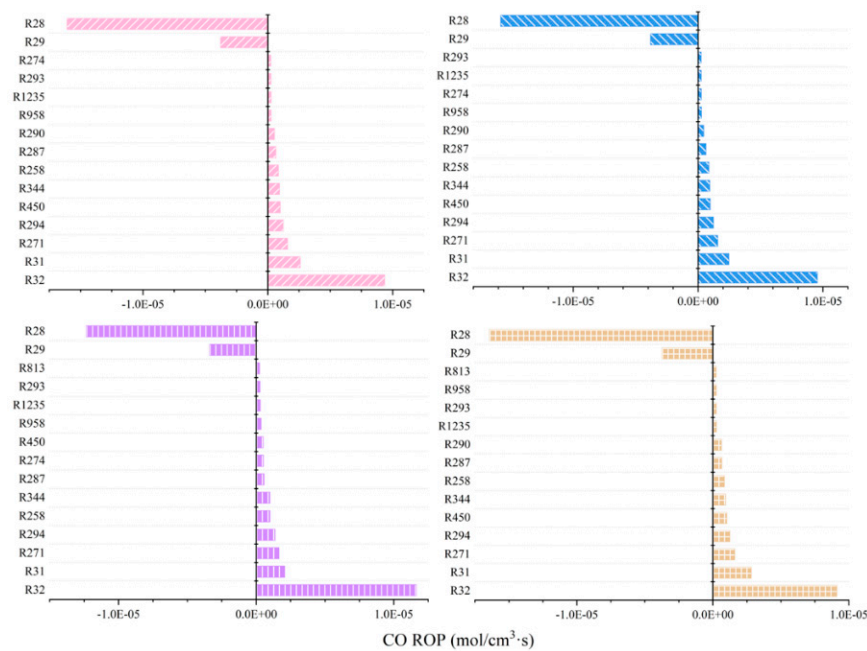


Figure 16. Comprehensive comparison of CO ROP of air–light hydrocarbon mixing gas at the maximum mixing degree for equivalence ratios of *n*-pentane.

Table 2. The key reactions for the production and annihilation of CO.

Number	Reaction	Number	Reaction
R1	$H + O_2 \rightleftharpoons O + OH$	R274	$CH_2CHO + O_2 \Rightarrow CH_2O + CO + OH$
R4	$O + H_2O \rightleftharpoons OH + OH$	R286	$CH_2CO + OH \rightleftharpoons HCCO + H_2O$
R12	$HO_2 + H \rightleftharpoons OH + OH$	R287	$CH_2CO + OH \rightleftharpoons CH_2OH + CO$
R13	$H + HO_2 \rightleftharpoons H_2 + O_2$	R290	$HCCO + OH \Rightarrow H_2 + CO + CO$
R14	$HO_2 + O \rightleftharpoons OH + O_2$	R293	$HCCO + O_2 \Rightarrow OH + CO + CO$
R15	$OH + HO_2 = H_2O + O_2$	R294	$HCCO + O_2 \Rightarrow CO_2 + CO + H$
R16	$OH + HO_2 = H_2O + O_2$	R301	$C_2H_4 + O \rightleftharpoons CH_3 + HCO$
R28	$CO + OH \rightleftharpoons CO_2 + H$	R302	$C_2H_4 + O \rightleftharpoons CH_2CHO + H$
R29	$CO + OH \rightleftharpoons CO_2 + H$	R303	$C_2H_4 + OH \rightleftharpoons C_2H_3 + H_2O$
R31	$HCO + M \rightleftharpoons H + CO + M$	R344	$C_2H_3 + O_2 = CH_2O + H + CO$
R32	$HCO + O_2 \rightleftharpoons CO + HO_2$	R450	$C_2H_3 + CO \rightleftharpoons C_2H_3CO$
R73	$CH_2O + OH \rightleftharpoons HCO + H_2O$	R670	$C_3H_6 + OH \rightleftharpoons C_3H_5-A + H_2O$
R78	$CH_2O + OH \rightleftharpoons HOCH_2O$	R813	$CHOCHO + OH \Rightarrow HCO + CO + H_2O$
R146	$CH_3 + HO_2 \rightleftharpoons CH_3O + OH$	R832	$C_3H_5-A + O \rightleftharpoons C_2H_3CHO + H$
R258	$CH_3CO (+M) \rightleftharpoons CH_3 + CO (+M)$	R958	$CH_3CHCO + OH \rightleftharpoons SC_2H_4OH + CO$
R271	$CH_2CHO (+M) \rightleftharpoons CH_3 + CO (+M)$	R1235	$CH_2CHCHCHO \rightleftharpoons C_3H_5-A + CO$

4. Conclusions

At atmospheric pressure, a detailed mechanism was used to study the ignition delay time, laminar flame speed, extinction residence time, and CO emission of air–light hydrocarbon mixing gas with different mixing degrees at the critical equivalence ratios. Comparing the ignition delay time of air–light hydrocarbon mixing gas with *n*-pentane, it was found that there is a temperature node of 1118 K. When the temperature is higher than this node, the ignition delay time of air–light hydrocarbon mixing gas is less than that of *n*-pentane, otherwise the reverse. The study of the laminar flame speed and the ignition delay time together discovered a substantial problem of air–light hydrocarbon mixing gas. Air–light hydrocarbon mixing gas is obtained by mixing *n*-pentane and air, thus its characteristic parameters are mainly determined by the ratio of *n*-pentane and total air. Regarding the relevant studies on the extinction residence time and the CO emission index, the minimum extinction residence time and the minimum CO emission index of air–light hydrocarbon mixing gas do not occur at the same mixing degree. The CO sensitivity analysis and the CO emission index indicate that, when the equivalence ratio is 1.7 and the maximum mixing degree of air–light hydrocarbon mixing gas is 1:3, the CO emission index is the highest for all air–light hydrocarbon mixing gas cases studied, and the key to the production of CO is the reaction $H + O_2 \rightleftharpoons O + OH$. The results of this study indicate that choosing an appropriate mixture degree of air–light hydrocarbon mixing gas at different equivalence ratios can indeed improve the combustion characteristics.

Author Contributions: Conceptualization, Z.M.; Methodology, Z.M.; Validation, J.W.; Formal analysis, Z.M., C.X., and J.Q.; Resources, J.W.; Writing—original draft preparation, Z.M.; Writing—review and editing, Z.M. and J.W.; Data curation, J.Q. and L.H.; Visualization, Z.M.; Software, Z.M.; Supervision, C.X. and J.Q.; Project administration, J.W. and L.H.; and Funding acquisition, J.W. All authors have read and agreed to the published version of the manuscript.

Funding: This work was supported by the Central Government of China Guides Special Foundation for Local Science and Technology Development (19944508G).

Acknowledgments: NUI Galway pentane isomer model was shared by National University of Ireland, Galway.

Conflicts of Interest: The authors declare no conflict of interest.

References

- Zhang, S.; Ma, B. Development Trend of World Energy and Future Development Directions of China's Energy. *Nat. Res. Econ. Chin.* **2019**, *32*, 20–27, 32.

2. Liang, H.; Li, Y. Countermeasures to risks of Chinese energy security under major changes of world petroleum pattern caused by uprising of the petroleum industry of USA. *Chin. Min. Mag.* **2019**, *28*, 7–12.
3. Zheng, C. *China Energy (Group) Top 500 Analysis Report*. China Energy News/2019/December/16th/Edition 004, CNKI, China. 2019. Available online: <https://kns.cnki.net/KCMS/detail/detail.aspx?dbcode=CCND&dbname=CCNDLAST2020&filename=SHCA201912160040&v=MDY0MDhIOWpOclki1RFpPc0xEQk5LdWhkaG5qOThUbmpxcXhkRWVNT1VcmlmWmVadkVddmk0> (accessed on 19 June 2020).
4. Yan, X.; Lu, G. *Perspective of China's Energy Strategy from the World Energy Trend*. China Energy News/2019/5/6/6/Edition 004, International, CNKI, China. 2019. Available online: <https://kns.cnki.net/KCMS/detail/detail.aspx?dbcode=CCND&dbname=CCNDLAST2019&filename=CKYB201905240080&v=MjJyMjRaT3NIREJOS3VoZGhuajk4VG5qcXF4ZEZVITU9VS3JpZlplWkZXJQZV1> (accessed on 19 June 2020).
5. Han, J.; Gao, R.; Zhang, S.; Zhang, Y. A Feasibility Study into Using Light-hydrocarbon Liquid from Remote Fields as Domestic Fuels. *Sino-Glob. Energy* **2012**, *17*, 90–94.
6. Fan, Y.; Wei, J.; Zhang, S.; Shi, D. Research on calculation method of the density of air-light hydrocarbon mixing gas. *Tech. Superv. Pet. Ind.* **2018**, *34*, 23–24, 28.
7. Fan, Y.; Shi, D.; Wei, J.; Zhang, S. Research on calculation method of the dew point of air-light hydrocarbon mixing gas. *Tech. Superv. Pet. Ind.* **2018**, *34*, 3–5.
8. Fan, Y.; Zhang, S.; Shi, D.; Wei, J. Research on calculation method of the explosion limit of air-light hydrocarbon mixing gas. *Tech. Superv. Pet. Ind.* **2018**, *34*, 40–42.
9. Xie, Y.; Wang, J.; Zhang, M.; Gong, J.; Jin, W.; Huang, Z. Experimental and numerical study on laminar flame characteristics of methane oxy-fuel mixtures highly diluted with CO₂. *Energy Fuels* **2013**, *27*, 6231–6237. [[CrossRef](#)]
10. Hu, E.; Huang, Z.; He, J.; Jin, C.; Zheng, J. Experimental and numerical study on laminar burning characteristics of premixed methane–hydrogen–air flames. *Int. J. Hydrog. Energy* **2009**, *34*, 4876–4888. [[CrossRef](#)]
11. Brower, M.; Petersen, E.L.; Metcalfe, W.; Curran, H.J.; Furi, M.; Bourque, G.; Aluri, N.; Güthe, F. Ignition delay time and laminar flame speed calculations for natural gas/hydrogen blends at elevated pressures. *J. Eng. Gas Turbines Power* **2013**, *135*. [[CrossRef](#)]
12. Wang, J.; Huang, Z.; Tang, C.; Miao, H.; Wang, X. Numerical study of the effect of hydrogen addition on methane–air mixtures combustion. *Int. J. Hydrog. Energy* **2009**, *34*, 1084–1096. [[CrossRef](#)]
13. Hu, F.; Li, P.; Guo, J.; Liu, Z.; Wang, L.; Mi, J.; Dally, B.; Zheng, C. Global reaction mechanisms for MILD oxy-combustion of methane. *Energy* **2018**, *147*, 839–857. [[CrossRef](#)]
14. Liu, J.; Zhang, X.; Wang, T.; Hou, X.; Zhang, J.; Zheng, S. Numerical study of the chemical, thermal and diffusion effects of H₂ and CO addition on the laminar flame speeds of methane–air mixture. *Int. J. Hydrog. Energy* **2015**, *40*, 8475–8483. [[CrossRef](#)]
15. Karyeyen, S. Combustion characteristics of a non-premixed methane flame in a generated burner under distributed combustion conditions: A numerical study. *Fuel* **2018**, *230*, 163–171. [[CrossRef](#)]
16. Yan, Y.; Wu, G.; Huang, W.; Zhang, L.; Li, L.; Yang, Z. Numerical comparison study of methane catalytic combustion characteristic between newly proposed opposed counter-flow micro-combustor and the conventional ones. *Energy* **2019**, *170*, 403–410. [[CrossRef](#)]
17. Chen, J.; Song, W.; Xu, D. Optimal combustor dimensions for the catalytic combustion of methane-air mixtures in micro-channels. *Energy Convers. Manag.* **2017**, *134*, 197–207. [[CrossRef](#)]
18. Xiao, H.; Valera-Medina, A.; Bowen, P.J. Study on premixed combustion characteristics of co-firing ammonia/methane fuels. *Energy* **2017**, *140*, 125–135. [[CrossRef](#)]
19. Ku, J.W.; Choi, S.; Kim, H.K.; Lee, S.; Kwon, O.C. Extinction limits and structure of counterflow nonpremixed methane-ammonia/air flames. *Energy* **2018**, *165*, 314–325. [[CrossRef](#)]
20. Pilcher, G.; Chadwick, J.D.M. Measurements of heats of combustion by flame calorimetry. Part 4—n-Pentane, isopentane, neopentane. *Trans. Faraday Soc.* **1967**, *63*, 2357–2361. [[CrossRef](#)]
21. Knox, J.H.; Kinnear, C.G. The mechanism of combustion of pentane in the gas phase between 250 and 400 C. *Proc. Symp. (Int.) Combust.* **1971**, *13*, 217–227. [[CrossRef](#)]
22. Hughes, R.; Simmons, R.F. The low-temperature combustion of n-pentane. *Proc. Symp. (Int.) Combust.* **1969**, *12*, 449–461. [[CrossRef](#)]
23. Westbrook, C.K.; Pitz, W.J.; Thornton, M.M.; Malte, P.C. A kinetic modeling study of n-pentane oxidation in a well-stirred reactor. *Combust. Flame* **1988**, *72*, 45–62. [[CrossRef](#)]

24. Chakir, A.; Belumam, M.; Boettner, J.C.; Cathonnet, M. Kinetic study of n-pentane oxidation. *Combust. Sci. Technol.* **1991**, *77*, 239–260. [[CrossRef](#)]
25. Zhukov, V.P.; Sechenov, V.A.; Starikovskii, A.Y. Self-ignition of a lean mixture of n-pentane and air over a wide range of pressures. *Combust. Flame* **2005**, *140*, 196–203. [[CrossRef](#)]
26. Bugler, J.; Marks, B.; Mathieu, O.; Archuleta, R.; Camou, A.; Grégoire, C.; Heufer, K.A.; Petersen, E.L.; Curran, H.J. An ignition delay time and chemical kinetic modeling study of the pentane isomers. *Combust. Flame* **2016**, *163*, 138–156. [[CrossRef](#)]
27. Bugler, J.; Rodriguez, A.; Herbinet, O.; Battin-Leclerc, F.; Togbé, C.; Dayma, G.; Dagaut, P.; Curran, H.J. An experimental and modelling study of n-pentane oxidation in two jet-stirred reactors: The importance of pressure-dependent kinetics and new reaction pathways. *Proc. Combust. Inst.* **2017**, *36*, 441–448. [[CrossRef](#)]
28. Kelley, A.P.; Smallbone, A.J.; Zhu, D.L.; Law, C.K. Laminar flame speeds of C5 to C8 n-alkanes at elevated pressures: Experimental determination, fuel similarity, and stretch sensitivity. *Proc. Combust. Inst.* **2011**, *33*, 963–970. [[CrossRef](#)]
29. Jiang, X.; Deng, F.; Yang, F.; Zhang, Y.; Huang, Z. High temperature ignition delay time of DME/n-pentane mixture under fuel lean condition. *Fuel* **2017**, *191*, 77–86. [[CrossRef](#)]
30. *Ansys Chemkin 17.0 (15151)*, ANSYS Reaction Design: San Diego, CA, USA, 2016.
31. Hui, X.; Zhang, C.; Xia, M.; Sung, C.-J. Effects of hydrogen addition on combustion characteristics of n-decane/air mixtures. *Combust. Flame* **2014**, *161*, 2252–2262. [[CrossRef](#)]
32. Chang, L.; Lin, Y.; Cao, Z.; Xu, L. A new simplified mechanism for combustion of RP-3/Jet-A kerosene. *Energy Source. Part A* **2020**, *42*, 676–687. [[CrossRef](#)]
33. Chang, L.; Lin, Y.; Cao, Z.; Xu, L. Effects of water vapor addition on NO reduction of n-decane/air flames. *Energy Source. Part A* **2019**, 1–15. [[CrossRef](#)]



© 2020 by the authors. Licensee MDPI, Basel, Switzerland. This article is an open access article distributed under the terms and conditions of the Creative Commons Attribution (CC BY) license (<http://creativecommons.org/licenses/by/4.0/>).